

PAPER

Impact of barrier thickness on gate capacitance—modeling and comparative analysis of GaN based MOSHEMTs

To cite this article: Kanjalochan Jena *et al* 2015 *J. Semicond.* **36** 034003

View the [article online](#) for updates and enhancements.

You may also like

- [AlGaIn/GaN Metal-Oxide-Semiconductor High Electron Mobility Transistor with Liquid Phase Deposited Al₂O₃ as Gate Dielectric](#)
Sarbani Basu, Pramod K. Singh, Po-Wen Sze et al.
- [Direct current performance and current collapse in AlGaIn/GaN insulated gate high-electron mobility transistors on Si \(111\) substrate with very thin SiO₂ gate dielectric](#)
M Lachab, M Sultana, H Fatima et al.
- [Integrated Monolithic Inverter Using Gate-Recessed GaN-Based Enhancement-Mode and Depletion-Mode Metal-Oxide-Semiconductor High-Electron Mobility Transistors](#)
Ching-Ting Lee, Hsin-Ying Lee and Jhe-Hao Chang

Impact of barrier thickness on gate capacitance—modeling and comparative analysis of GaN based MOSHEMTs

Kanjalochoan Jena, Raghunandan Swain, and T. R. Lenka[†]

Department of Electronics and Communication Engineering, National Institute of Technology Silchar, Assam, 788010, India

Abstract: A mathematical model is developed predicting the behavior of gate capacitance with the nanoscale variation of barrier thickness in AlN/GaN MOSHEMT and its effect on gate capacitances of AlInN/GaN and AlGaIn/GaN MOSHEMTs through TCAD simulations is compared analytically. AlN/GaN and AlInN/GaN MOSHEMTs have an advantage of a significant decrease in gate capacitance up to $108 \text{ fF}/\mu\text{m}^2$ with an increase in barrier thickness up to 10 nm as compared to conventional AlGaIn/GaN MOSHEMT. This decrease in gate capacitance leads to improved RF performance and hence reduced propagation delay.

Key words: 2DEG; GaN; MOSHEMT; quantum capacitance; TCAD

DOI: 10.1088/1674-4926/36/3/034003 **EEACC:** 2570

1. Introduction

GaN-based MOSHEMTs (metal–oxide–semiconductor high electron mobility transistors) are getting more attention these days because of their low gate leakage current and improved gate capacitance due to the suitable material properties of GaN. When the device dimensions are reduced for a silicon based MOSFET (metal–oxide–semiconductor field effect transistor), it has become very difficult to reduce the other parameters like barrier potential, critical electric field, threshold voltage, etc., resulting short channel effects. Although many solutions have been proposed to overcome these limitations, researchers are very much interested in the use of new materials and technology that can improve the performance of electronic systems. However, research is progressing towards improving carrier transport in the transistor channel region. Among the various candidates, a high electron mobility based GaN channel MOSHEMT can overcome the short channel effects more than the traditional silicon MOSFET.

One of the main characteristics of MOSHEMTs is the capacitance formed between the gate and channel. However, for improved RF performance, less gate capacitance is required^[1,2]. For a scaled MOSHEMT, the gate capacitance is a series combination of oxide capacitance and channel or quantum capacitance (QC). The former is large due to a thinner oxide layer and has a higher value of dielectric constant, which means that QC will be the dominant source of gate capacitance^[3]. GaN based MOSHEMT with an AlN barrier layer over the GaN channel has attracted great interest due to the large difference in spontaneous and piezoelectric polarization, which results in a higher 2DEG density at the heterointerface.

It provides a large band offset with respect to GaN, resulting in the formation of a deep quantum well leading to a better carrier confinement^[4]. As a result, it does not suffer from large scattering, and a relatively small QC is associated with the channel. The limits imposed by the QC on the gate capacitance can be improved by barrier thickness scaling.

The compact charge based model for capacitance–voltage (C – V) characteristics in AlGaIn/GaN HEMT has already been presented considering all non ideal effects^[3,5,6]. However, the unavailability of a proper model explaining these phenomena for MOSHEMTs in the literature is the main driving force behind this work.

2. Comparison of heterostructures

For an unintentionally doped AlGaIn/GaN MOSHEMT structure, the two dimensional electron gas (2DEG) is formed largely as a result of piezoelectric and spontaneous polarization effects which arise at the heterointerface of the AlGaIn and GaN layers. However, for scaled devices, as the oxide thickness and gate lengths are reduced, barrier thickness scaling is necessary. While attempting to reduce the thickness of the AlGaIn barrier to overcome short channel effects, the sheet carrier density decreases due to the proximity of the heterointerface to the negatively charged surface^[7]. In order to further increase the 2DEG density as well as the breakdown field in the AlGaIn structure, a high Al mole fraction is desirable to increase the strength of polarization. However, a high Al content will result in poor transport properties in the AlGaIn/GaN heterostructure^[8].

In order to solve this problem, a thin lattice matched $\text{Al}_{0.83}\text{In}_{0.17}\text{N}$ layer is grown over the GaN, which eliminates the strain present in the conventional AlGaIn based MOSHEMT. The band gap of the AlInN is larger than that of a typical AlGaIn and has a larger spontaneous polarization charge as well. The larger bandgap results in an enhancement of the carrier confinement in the well, thus keeping the output resistance of the device high. The larger number of carriers tend to accumulate in the 2DEG, which results in a larger sheet carrier density and a correspondingly larger current and power densities than those that of the conventional AlGaIn/GaN system. However, in the case of an AlInN heterostructure, local in-homogeneity in the composition yields regions of increased alloy scattering due to the enhanced penetration of the electron

[†] Corresponding author. Email: trlenka@gmail.com

Received 27 July 2014, revised manuscript received 21 October 2014

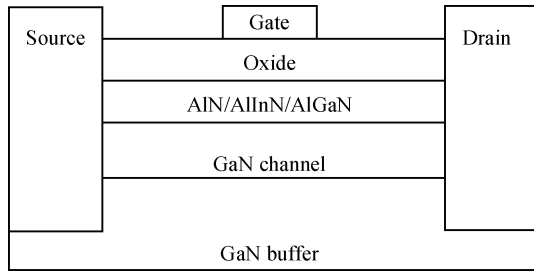


Figure 1. Proposed MOSHEMT structure.

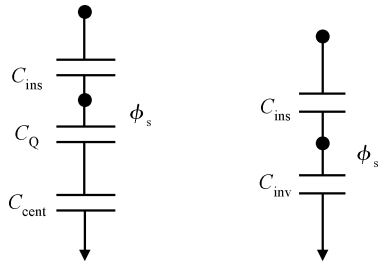


Figure 2. Equivalent circuit diagrams for gate capacitance in AlN/GaN MOSHEMT.

wave function into the barrier layer. Therefore, the AlInN barrier layer would be the best if it is uniform^[9].

To overcome these problems, AlN/GaN MOSHEMT can be an alternative candidate for high power applications. The 2DEG, which forms near the AlN/GaN interface, can reach up to a concentration of $3 \times 10^{13} \text{ cm}^{-2}$ for an extremely thin AlN barrier layer even less than 5 nm thickness along with high mobility greater than $1000 \text{ cm}^2/(\text{V}\cdot\text{s})$ ^[10].

3. Quantum capacitance

Figure 1 shows a schematic diagram of the AlN/GaN heterostructure used in this study. It consists of a metal gate followed by Al_2O_3 of thickness 1 nm, an AlN barrier layer, an unintentionally doped GaN channel of thickness 500 nm, and a GaN semi-insulating buffer layer of thickness $1 \mu\text{m}$. The total gate capacitance of the AlN/GaN MOSHEMT can be expressed as a series combination of insulator capacitance, C_{ins} and inversion capacitance, C_{inv} ^[11]. As per assumption, when the first electron sub-band in the channel is occupied, the inversion layer capacitance can be represented as a series of the quantum capacitance, C_Q and the centroid capacitance C_{cent} ^[11].

From Figure 2, it is well understood that the total gate capacitance (C_G) can be determined by the smallest gate capacitance component among the three of C_{ins} , C_Q and C_{cent} . The insulator capacitance is inversely proportional to the insulator thickness. Ideally, the inversion layer capacitance is much larger than the insulator capacitance in the strong inversion and gate capacitance approaches the insulator capacitance in large scaled devices.

However, in nano-scale devices, as insulator thickness approaches the nanometer range, the insulator capacitance becomes comparable to the inversion layer capacitance, which means that the quantum capacitance, C_Q , and the centroid capacitance, C_{cent} , start to affect the gate capacitance. The cen-

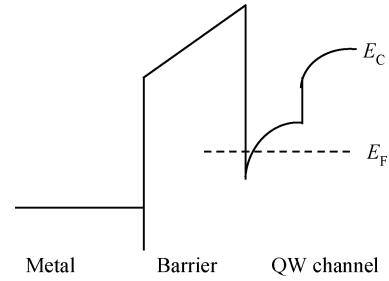


Figure 3. Conduction band diagram in strong inversion.

troid capacitance is related to the average physical distance of the electrons present in the quantum well from the metal gate^[12]. As in the case of AlN/GaN, the carriers are better confined in the quantum well, all charges can be assumed to be located at same position inside the quantum well and centroid capacitance can be neglected.

The QC was first introduced by Luryi^[13] and it originates from the penetration of the Fermi energy level (E_F) into the conduction energy band. Therefore, the channel material plays a very significant role for determining quantum capacitance.

In AlN/GaN MOSHEMT, a 2DEG is created in the heterostructure quantum well (QW) due to the finite density of states (DOS). As a result, the Fermi level needs to move upward above the conduction energy band edge as the charge in the quantum well increases. This movement of the Fermi level requires energy and this conceptually corresponds to QC. To induce channel charge in a MOS structure, we need to deliver an amount of energy equal to $Q_s^2/2C_{\text{ins}} + Q_s^2/2C_Q$ ^[12], where Q_s is the total electronic charge in 2DEG. The first term corresponds to the required energy for the electric field in the oxide layer and the second term is related to the required energy to create 2DEG. However, as C_{ins} is comparable even more than C_Q as the device scaling approaches a few nanometers, C_Q should be considered carefully in the scaled down devices to indicate gate capacitance. The problem is especially severe in III-V MOSHEMTs due to their relatively small effective mass, which reduces the QC.

4. Model development

For a MESFET/HEMT, the sheet charge concentration is given by^[4, 14]

$$n_s = \sigma_{\text{pol}} - \frac{\epsilon_{\text{AlN}}}{qd_{\text{AlN}}} (\phi_s + E_F - \Delta E_C), \quad (1)$$

where σ_{pol} is the induced charge concentration due to spontaneous polarization, ϵ_{AlN} is the permittivity for AlN, d_{AlN} is the barrier thickness, E_F is the Fermi potential in the GaN layer, ϕ_s is the surface potential and ΔE_C is the discontinuity of the conduction energy band at the heterointerface of AlN and GaN layers.

4.1. Dependence of n_s on barrier thickness

Figure 4 demonstrates the energy band diagram of a MOSHEMT structure. All the levels above the neutral level are acceptor states and below it are the donor states.

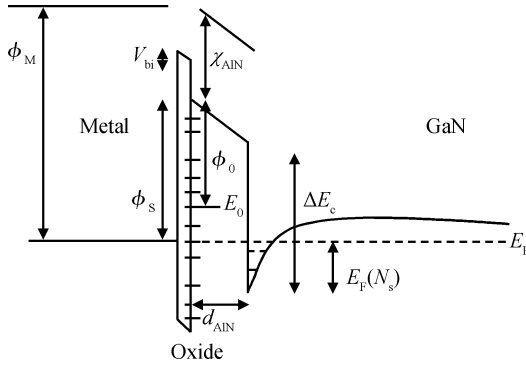


Figure 4. Conduction energy band profile for a metal/oxide/AlN/GaN interface.

As per the classical approach, all the levels above the Fermi level are considered to be devoid of electrons i.e. donors, while those below are filled. This results in the ionized state of the donor traps while the acceptor traps are neutral. It results in an extra positive interface charge contributed by these states, which can be given by^[4]

$$Q_{it} = D_{it}q^2 (E_0 - E_F). \quad (2)$$

Here D_{it} is the interface density of states. Q_{it} is the interface charge, E_0 and E_F are the neutral and Fermi level potentials respectively, which denotes that all the states between E_0 and E_F are ionized.

This donor charge along with the polarization charge results in a residual potential V_{bi} , which can be given by

$$V_{bi} = \frac{Q_D + Q_{it}}{C_{oxide}}, \quad (3)$$

where Q_D is the depletion charge and C_{oxide} is the oxide capacitance. The depletion charge can be formulated as

$$Q_D = qN_Dd_{AIN}. \quad (4)$$

Making use of Equations (2), (3) and (4), we get

$$V_{bi} = \frac{qN_Dd_{AIN} + D_{it}q^2 (E_0 - E_F)}{C_{oxide}}. \quad (5)$$

Clearly from Figure 4 we see that the surface potential $\phi_s = \phi_M - \chi_{AIN} - V_{bi}$ and $E_0 - E_f = \phi_s - \phi_0$ where ϕ_M is the metal work function, χ_{AIN} is the electron affinity for AlN, V_{bi} is the residual interface potential and ϕ_0 is the potential difference between the neutral level and the conduction band edge. Introducing these relations in Equation (5), we get a relation between the surface potential and barrier thickness

$$\phi_s = \gamma (\phi_M - \chi_{AIN}) + (1 - \gamma) \phi_0 - \frac{\gamma q N_D d_{AIN}}{C_{oxide}}, \quad (6)$$

where $\gamma = \frac{1}{1 + D_{it}q^2/C_{oxide}}$.

The dependence of 2DEG sheet charge density on the surface potential and the dependence of thickness on surface potential can be seen from Equations (1) and (6). Making use of

these equations we will get the 2DEG sheet charge density^[4] as per Equation (7).

$$n_s = \sigma_{pol} - \frac{\epsilon_{AIN}}{qd_{AIN}} \left[\gamma (\phi_M - \chi_{AIN}) + (1 - \gamma) \phi_0 - \frac{\gamma q N_D d_{AIN}}{C_{oxide}} + E_F - \Delta E_C \right]. \quad (7)$$

Taking the solution of the Schrödinger and Poisson equations^[1,2] into consideration, provided only two levels (E_0 and E_1) in the two dimensional triangular potential well are to be occupied, gives us the following relation^[4, 15].

$$n_s = DkT \sum_{i=0,1} \ln \left(1 + \exp \frac{E_F - E_i}{kT/q} \right), \quad (8)$$

where $D = 4\pi m^*/h^2$ is the conduction band density of states of a 2-D system, m^* is the electron effective mass, h is the Planck constant, k is the Boltzmann constant, T is the ambient temperature, $E_0 = c_0 n_s^{2/3}$ (in eV), and $E_1 = c_1 n_s^{2/3}$ (in eV) are the allowed energy levels in the well. Here c_0 and c_1 are determined by the Robin boundary condition^[16, 17].

However, the Fermi level can be expressed by a 2nd order expression as per Kola *et al.*^[17], which gives a good fitting to the numerical solution of Equation (8), where E_F is given by

$$E_F = k_1 + k_2 n_s^{1/2} + k_3 n_s, \quad (9)$$

where k_1, k_2 and k_3 have been calculated by Li *et al.*^[16]. Making use of Equations (9) and (7) and solving for n_s we get

$$n_s = \left[-A + \sqrt{A^2 - (B + C\phi_s - F)} \right]^2, \quad (10)$$

where

$$A = \frac{\epsilon k_2}{2(\epsilon k_3 + qd)}, \quad (11)$$

$$B = \frac{\epsilon(k_1 - \Delta E_C)}{(\epsilon k_3 + qd)}, \quad (12)$$

$$C = \frac{\epsilon}{\epsilon k_3 + qd}, \quad (13)$$

$$F = \frac{dq\sigma}{\epsilon k_3 + qd}. \quad (14)$$

4.2. Dependence of gate capacitance on barrier thickness

Now neglecting the centroid capacitance, the QC can be obtained as

$$QC = \frac{\partial (qn_s)}{\partial \phi_s}. \quad (15)$$

Calculating the above differentiation, we will find

$$QC = q \frac{C \left[-A + \sqrt{A^2 - (B + C\phi_s - F)} \right]}{\sqrt{A^2 - (B + C\phi_s - F)}}. \quad (16)$$

Now the gate capacitance due to the series combination of C_Q and C_{ox} can be written as

$$C_G = \frac{QC \times C_{ox}}{QC + C_{ox}}. \quad (17)$$

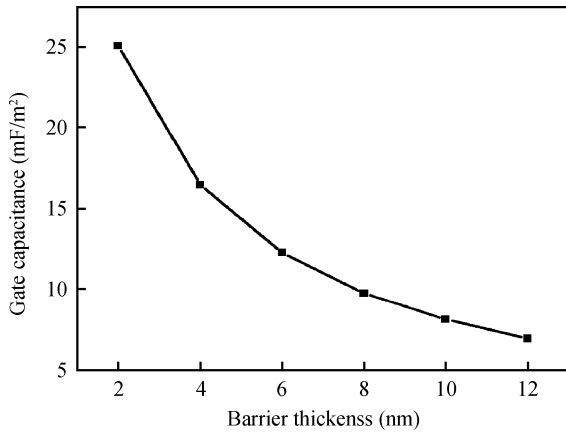


Figure 5. Plot showing gate capacitance versus barrier thickness for AlN/GaN MOSHEMT.

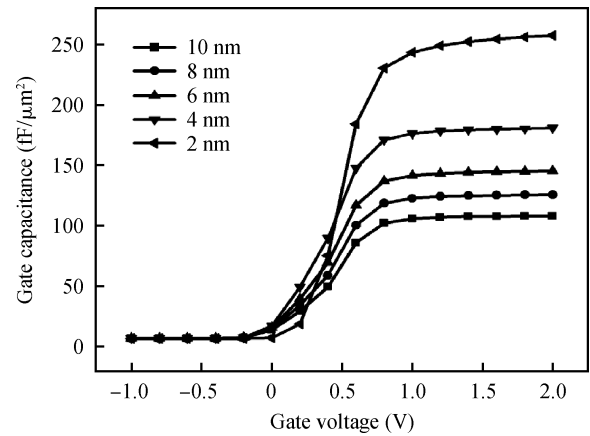


Figure 6. Plot showing gate capacitance versus gate voltage for different barrier thicknesses of AlN/GaN MOSHEMT.

Table 1. List of model parameters.

Parameter	Description	Value
ϵ_{AlN}	Permittivity of AlN layer	$10.78\epsilon_0 \text{ F/m}^2$
$\epsilon_{\text{Al}_2\text{O}_3}$	Permittivity of Al_2O_3 layer	$9.1\epsilon_0 \text{ F/m}^2$
ϵ_{GaN}	Permittivity of GaN layer	$9.8\epsilon_0 \text{ F/m}^2$
K_1	Subthreshold factor	-0.0802 V
K_2	Linear factor	$1.039 \times 10^{-9} \text{ V/m}$
K_3	Saturation factor	$1.0454 \times 10^{-18} \text{ V/m}^2$
q	Electronic charge	$1.69 \times 10^{-19} \text{ C}$
C_0	Experimental parameter	2.5×10^{-12}
C_1	Experimental parameter	3.2×10^{-12}
$\Delta E_{C(\text{AlN})}$	Conduction band discontinuity	0.343 eV
σ_{pol}	Spontaneous polarization charges	$3.38 \times 10^{17} \text{ m}^{-2}$
t_{oxide}	Oxide thickness	6 nm
ϕ_s	Surface Potential of AlN	1.9 eV
ϕ_M	Metal work function	4.3 eV
χ_{AlN}	Electron affinity of AlN	0.6 eV
N_D	Doping concentration	$1.5 \times 10^{16} \text{ m}^{-3}$
D_{it}	Density of states	$1.2 \times 10^{12} \text{ m}^{-3}$

Then Equation (17) is plotted in MATLAB by taking the necessary parameters for AlN/GaN MOSHEMT to see graphically the dependence of gate capacitance on barrier thickness, as shown in Figure 5. The parameters are taken from the existing literature and are mentioned in Table 1. It is observed from this figure that with an increase in barrier thickness, the capacitance decreases which can be justified by TCAD simulation results, as shown in the next section.

5. Simulation results and discussion

This section illustrates the simulation study, carried out using the Atlas TCAD tool^[18]. In the following analysis, different parameters such as temperature at 300 K, step gate voltage as 0.2 V, with an initial gate voltage of -1 V and the final gate

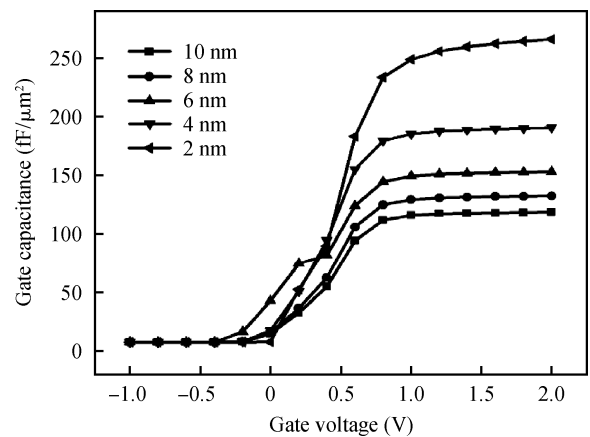


Figure 7. Plot showing gate capacitance versus gate voltage for different barrier thicknesses of $\text{Al}_{0.83}\text{In}_{0.17}\text{N}/\text{GaN}$ MOSHEMT.

voltage of 2 V at applied 1 V drain bias voltage for a 50 nm gate length device are considered, which are kept the same for all three devices with various barrier thicknesses of $2, 4, 6, 8$ and 10 nm .

The simulation results of gate capacitance with respect to the gate voltage for various barrier thicknesses in AlN/GaN, AlInN/GaN and AlGaIn/GaN MOSHEMTs are shown in Figures 6, 7 and 8 respectively. It is observed from these figures that as the barrier thickness increases from 2 to 10 nm , the gate capacitance decreases significantly with the increase in gate voltage. However, at a very low gate voltage such as at -0.8 V and -1 V , the value of the gate capacitance is almost the same for all barrier thicknesses. However, in AlGaIn/GaN MOSHEMT, the decrease of the gate capacitance is much less significant.

In Figure 9, the gate capacitance for different barrier thicknesses at gate voltage of 1 V is shown. It is observed here that at a particular barrier thickness, the gate capacitance is the lowest for AlN/GaN MOSHEMT than the other two cases and highest for AlGaIn/GaN MOSHEMT. It can be explained here that in AlN/GaN MOSHEMT, the 100% Al content leads to more of a polarization effect and more charge carrier confinement resulting in less density of states near the quantum well, leading to less QC. However, in $\text{Al}_{0.83}\text{In}_{0.17}\text{N}/\text{GaN}$ and

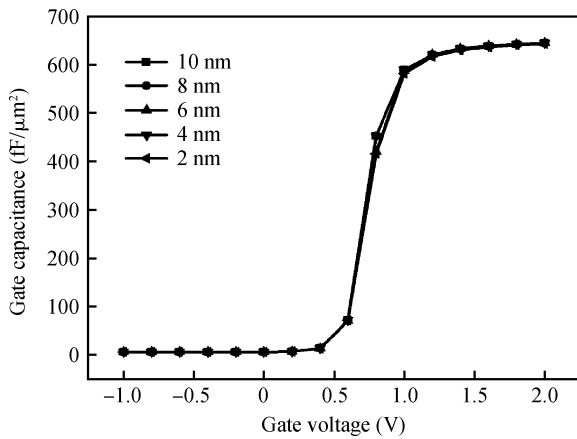


Figure 8. Plot showing gate capacitance versus gate voltage for different barrier thicknesses of AlGaIn/GaN MOSHEMT.

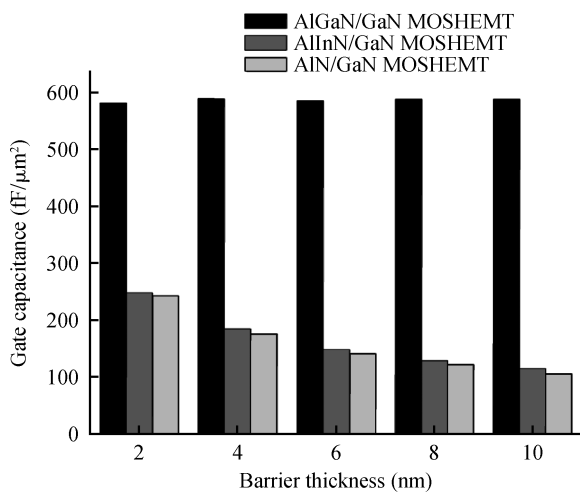


Figure 9. Plot showing gate capacitance versus barrier thickness.

$\text{Al}_{0.3}\text{Ga}_{0.7}\text{N}/\text{GaN}$ HEMT structures, the Al content is 83% and 30% respectively, which results in a comparatively lower polarization effect and less carrier confinement leading to more QC and hence more gate capacitance.

Modeling of quantum capacitance shows that it depends upon the properties of the barrier material and as we increase the Al content, the QC reduces and as it is in series with oxide capacitance, then it cannot be neglected in scaled down devices.

6. Conclusion

In this paper, we have observed the effect of the variation of barrier thickness on gate capacitance at different gate voltages for (AlN/GaN, AlInN/GaN, AlGaIn/GaN) MOSHEMT structures through a suitable modeling and extensive TCAD device simulations. After the comparison and analysis, we conclude here that in the nanometer regime, AlN/GaN and AlInN/GaN MOSHEMTs show better performance over the conventional AlGaIn/GaN MOSHEMT due to less quantum capacitance. Hence it improves the cut-off frequency for RF applications, threshold voltage, and reduces the gate leakage current.

Acknowledgement

The authors acknowledge the Microelectronics Computational Lab of the Department of Electronics and Communication Engineering of the National Institute of Technology Silchar, India for providing all the necessary facilities to carry out the research work.

References

- [1] Lenka T R, Panda A K. Role of nanoscale AlN and InN for the microwave characteristics of AlGaIn/(Al, In)N/GaN-based HEMT. *Semiconductors*, 2011, 45(9): 1211
- [2] Lenka T R, Dash G N, Panda A K. RF and microwave characteristics of 10 nm thick InGaIn-channel gate recessed HEMT. *Journal of Semiconductors*, 2013, 34(11): 1140031
- [3] John D L, Castro L C, Pulfrey D L. Quantum capacitance in nano scale device modeling. *Appl Phys Lett*, 2004, 96(9): 5180
- [4] Pandey D, Lenka T R. Model development for analyzing 2DEG sheet charge density and threshold voltage considering interface DOS for AlInN/GaN MOSHEMT. *Journal of Semiconductors*, 2014, 35(10): 104001
- [5] Yigletu F M, Khandelwal S, Fjeldly T A, et al. Compact charge-based physical models for current and capacitances in AlGaIn/GaN HEMTs. *IEEE Trans Electron Devices*, 2013, 60(11): 3746
- [6] Khandelwal S, Fjeldly T A. A physics based compact model of $I-V$ and $C-V$ characteristics in AlGaIn/GaN HEMT devices. *Solid State Electron*, 2012, 76: 60
- [7] Higashiwaki M, Matsui T, Mimura T. AlGaIn/GaN MIS-HEMTs with f_T of 13 GHz using cat-CVD SiN gate-insulating and passivation layers. *IEEE Electron Device Lett*, 2006, 27(1): 16
- [8] Nakamura F, Hashimoto S, Hara M, et al. AlN and AlGaIn growth using low-pressure metal-organic chemical vapor deposition. *J Cryst Growth*, 1998, 195(4): 280
- [9] Medjdoub F, Alomari M, Carlin J F, et al. Barrier layer scaling of InAlN/GaN HEMTs. *IEEE Electron Device Lett*, 2008, 29(5): 422
- [10] Dabiran A M, Wowchak A M, Osinsky A, et al. Very high channel conductivity in low-defect AlN/GaN high electron mobility transistor structures. *Appl Phys Lett*, 2008, 93(8): 082111
- [11] Takagi S, Toriumi A. Quantitative understanding of inversion-layer capacitance in Si MOSFET's. *IEEE Trans Electron Devices*, 1995, 42(12): 2125
- [12] Pal S, Cantely K D, Ahmed S S, et al. Influence of band structure and channel structure on the inversion layer capacitance of silicon and GaAs MOSFETs. *IEEE Trans Electron Devices*, 2008, 55(3): 904
- [13] Luryi S. Quantum capacitance devices. *Appl Phys Lett*, 1988, 52(6): 501
- [14] Ambacher O, Smart J, Shealy J R, et al. Two-dimensional electron gases induced by spontaneous and piezoelectric polarization charges in N and Ga-face AlGaIn/GaN hetero structures. *Appl Phys Lett*, 1999, 85(6): 3222
- [15] Kola S, Golio J M, Maracas G N. An analytical expression for Fermi level versus sheet carrier concentration for HEMT modeling. *IEEE Electron Device Lett*, 1988, 9(3): 136
- [16] Li M, Wang Y. 2-D analytical model for current-voltage characteristics and transconductance of AlGaIn/GaN MODFETs. *IEEE Trans Electron Devices*, 2008, 55(1): 261
- [17] Cheng X, Li M, Wang Y. Physics-based compact model for AlGaIn/GaN MODFETs with close formed $I-V$ and $C-V$ characteristics. *IEEE Trans Electron Devices*, 2009, 56(12): 2881
- [18] ATLAS User's Manual of SILVACO Inc, Ver. 5.12.0.R, 2010